Stem Cell Reports, Volume *6*

Supplemental Information

Lysophosphatidic Acid Receptor Is a Functional Marker of Adult Hippocampal Precursor Cells

Tara L. Walker, Rupert W. Overall, Steffen Vogler, Alex M. Sykes, Susann Ruhwald, Daniela Lasse, Muhammad Ichwan, Klaus Fabel, and Gerd Kempermann

Supplemental Figures

Figure S1, related to Figure 1. Coronal brain sections from an adult LPA_1-GFP mouse

Panel of representative coronal cryosections from a one-in-three series cut at a thickness of 20 µm. The endogenous GFP signal was amplified by additional staining using an anti-GFP-antibody.

Figure S2, related to Figure 1. LPA_1-GFP cells are also found in other brain regions

(a) GFP^+ cells are visible in the CA3 region of the hippocampus. (b) Prominent GFP signal is observed in the vasculature (green) in the hippocampal fissure, PROX-1 (red). (c) In the adult SVZ, the ventricular lining and only a few cells show a faint GFP signal. No overlap with BrdU (blue) and DCX (red) is observed. (d, d*) GFP signal compared to GFP immunofluorescence (Cy5 colored green; d*) in the SVZ. (e) GFP^+ cells in the glomeruli of the olfactory bulb co-express TBR2 (red). (f) GFP^+ cells in the olfactory bulb show no obvious co-localization to either DCX (f, red) or Calretinin (f, blue) but co-localize with SOX2 (g, red). The cortex (at the level of the SVZ) shows a population of GFP^+ cells that has no obvious co-localization with TBR2 (h, red), but an overlap with NeuN expression (h*, red). (i) A population of bright GFP^+ cells is visible in the habenula (SOX2, red). Scale bars are 100 µm in b, d and d* and 25 µm in f, g; all others are 50 µm. Panels d, d*, e, h* and i are maximum intensity projections and panels c, f, g and h are single planes of z-stacks.

Figure S3, related to Figure 3. Additional markers in combination with LPA_1-GFP allow the proliferative precursor population to be isolated

(a) A histogram representing the number of neurospheres generated per 1000 cells from the LPA_1-GFP^{high} and LPA_1-GFP^{low} populations. Data represent the mean ± SEM from 3 independent experiments, * $p = 0.05$, Student's t-test. (b) A histogram representing the neurosphere-forming capacity of the four cell populations isolated on the basis of LPA_1-GFP and EGFR expression. Data represent the mean ± SEM from 3 independent experiments, $F_7 = 38.2$, ** $p = 0.002$, one-way ANOVA with Tukey's multiple comparison test. (c) A histogram representing the neurosphere-forming capacity of the three cell populations isolated on the basis of LPA_1-GFP, EGFR and prominin-1 (CD133) expression. Data represent the mean ± SEM from 3 independent experiments, $F_7 = 26.8$, *** $p = 0.001$, one-way ANOVA with Tukey's multiple comparison test.

Figure S4, related to Figure 4. The LPA_1^+ precursor cell population does not contain any contaminating blood or endothelial cells

Primary dentate gyrus cells from LPA_1-GFP mice were gated on the basis of forward and side scatter and separated into LPA_1-GFP^+ and LPA_1-GFP^- populations: isotype-PE controls were used to set the background gates (a). (b) Whereas a small percentage of $CD31^+$ endothelial cells were present in the LPA_1-GFP^- population (3 %), no CD31-PE^+ cells were detected in the LPA_1-GFP^+ population (<1 %). Compared to the APC isotype control (c) no $CD45^+$ lymphocytes could be found in the LPA_1-GFP^+ population (<0.1 %) and only a small percentage in the LPA_1-GFP^- population (3 %; d).

Figure S5, related to Figure 4. CXCL1 increases primary hippocampal and SVZ neurosphere number

Significantly more neurospheres were generated from primary dentate gyrus (a) and SVZ (b) cells in the presence of the cytokine CXCL1. In contrast, no effect on neurosphere number was observed when cells from either region were cultured in the presence of CXCL2 or CCL8 (c-f). Data represent the mean ± SEM from 3 independent experiments, * $p < 0.05$, ** $p < 0.01$, two-sided Student's t-test.

Table S1, related to Figure 4. List of precursor cell specific genes

Lists of genes which were expressed at levels 4-fold higher (log_2 difference greater than 2) in the LPA_1^+ populations vs. the LPA_1^+ population "precursor cell specific"

Table S2, related to Figure 4. List of proliferative cell specific genes

Lists of genes which were expressed at levels 4-fold higher (log_2 difference greater than 2) in the $LPA_1^+EGFR^+prominin\text{-}1^+$ population vs. the other two populations "Proliferative cell specific".

Table S3, related to Figure 4. Gene Ontology enrichment analysis of the precursor cell populations

Results of a Gene Ontology enrichment analysis of the 255 precursor cell specific genes ("LPA1-positive cell specific" from Table S1). The *p*-values are given for a Fisher test as well as after Benjamini-Hochberg correction ("adjP"). Only results that were significant (adjP < 0.05) after correction are shown.

Table S4, related to Figure 4. Gene Ontology enrichment analysis of the proliferative cell population

Results of a Gene Ontology enrichment analysis of the 145 precursor cell specific genes ("Proliferative cell specific" from Table S1). The *p*-values are given for a Fisher test as well as after Benjamini-Hochberg correction ("adjP"). Only results that were significant (adjP < 0.05) after correction are shown.

List of primary antibodies

Antibody	Species	Dilution	Company	Catalog number
βIII-tubulin	mouse	1:2000	Promega	G712A
BrdU	rat	1:500	AdD Serotec	OBT0030
BrdU	mouse	1:500	BD Bioscience	347580
Calretinin	mouse	1:250	Swant	6B3
DCX	goat	1:250	Santa Cruz	sc-8066
FOX3	rabbit	1:500	Abcam	ab104225
GFAP	mouse	1:1000	Sigma	63893
GFAP	rabbit	1:500	DakoCytomation	z0334
GFP	rabbit	1:400	Invitrogen	A11122
MAP2ab	mouse	1:200	Sigma	M1406
Nestin	mouse	1:200	BD Biosciences	611658
NeuN	mouse	1:100	Chemicon	MAB377
NeuroD	goat	1:250	Santa Cruz	sc-1086
O4	mouse	1:100	R&D Systems	MAB1326
Prominin-1-PE	mouse	1:200	eBioscience	12-1331
SOX2	goat	1:400	Santa Cruz	sc-17320
s100β	rabbit	1:800	Abcam	ab52642
TBR2	rabbit	1:800	Abcam	ab23345
Vimentin	chicken	1:2000	Millipore	AB5733

Supplemental Experimental Procedures

Animals

Frozen sperm of LPA_1-GFP mice (FVB/N-Swiss Webster background) were obtained from the GENSAT organization (Gong et al., 2003) and transferred to C57BL/6 female mice by laser-assisted *in vitro* fertilization resulting in LPA_1-GFP mice with a mixed FVB/N-Swiss Webster-C57BL/6 background. Only male animals were positive for GFP and were crossed to wild-type littermates. Nestin-GFP mice (Yamaguchi et al., 2000) were generated by Masuhiro Yamaguchi (University of Tokyo, Japan). Nestin-Cyan nuclear mice (Encinas and Enikolopov, 2008) were provided by Grigori Enikolopov (Cold Spring Harbor Laboratories, NY, USA). All experiments were conducted in accordance with the applicable European and National regulations (Tierschutzgesetz) and approved by the responsible authority (Landesdirektion Sachsen). Animals were maintained on a 12 h light/dark cycle with food and water provided *ad libitum*. All animals were 8 weeks old at the time of the experiment and the cohorts consisted of a mixture of male and females. For detection of proliferation in running LPA_1-GFP mice, animals were housed in pairs for 10 d in cages in the presence or absence of running wheels (TSE, Germany).

Brain tissue preparation

LPA_1-GFP mice (8 weeks) were perfused transcardially with 0.9 % NaCl followed by 4 % paraformaldehyde (PFA). The brains were then removed and postfixed in 4 % PFA overnight. After postfixation, the brains were cryoprotected by incubation overnight in 30 % w/v sucrose in phosphate buffered saline (PBS) until they sank. Frozen coronal serial sections (40 µm) were cut using a dry-ice cooled copper stage at a Leica table-top sliding microtome and stored at 4 °C in cryoprotectant solution (25 % ethyleneglycol, 25 % glycerol in 0.1 M phosphate buffer pH 7.4). Another set of brains was specifically processed for whole section imaging. These brains were cut to 20 µm thickness using a CryoStar NX70 Cryostat (Thermo Scientific) and kept at 4 °C until further processing.

BrdU and GFP immunohistochemistry (DAB)

For quantification of $BrdU^+$ and GFP^+ cells in the dentate gyrus, sections were treated with 0.6 % H_2O_2 in order to block endogenous peroxidase activity, washed and incubated in pre-warmed 2 N HCl (37 °C) washed in tris buffered saline (TBS), blocked in a solution containing 10 % normal donkey serum (NDS; Sigma-Aldrich) in 0.1 M TBS containing 0.2 % Triton-X-100 and incubated with BrdU (1:500; BD Bioscience) or GFP antibody (1:400; Invitrogen) in TBS containing 3 % NDS with 0.2 % Triton X-100 overnight at 4 °C. The sections were then washed and incubated for 4 h with anti-rat-biotin secondary antibody (Dianova), washed again and incubated in Vectastain ABC-Elite reagent (9 µg/ml, Vector Laboratories, LINARIS Germany) for 1 h, washed and 0.075 mg/ml diaminobenzidine (DAB; Sigma, Germany) with 0.04 % NiCl applied as the chromogen. Every sixth section (240 µm apart) was counted in the complete ventral dorsal extent of the dentate gyrus by brightfield microscopy at 40x magnification using a Leica DM 750 microscope. Results were multiplied by 6 in order estimate the total number of cells per dentate gyrus.

CldU, IdU and NeuN fluorescence immunohistochemistry

Sections were first washed with PBS and treated with 0.9 % NaCl, before DNA denaturation was performed in 2 N HCl for 30 min at 37 °C. The sections were then thoroughly washed with PBS and blocked for 1 h in PBS supplemented with 10 % donkey serum (Jackson ImmunoResearch Laboratories Inc) and 0.1 % Triton X-100. Primary antibodies (rat anti-BrdU, mouse anti-BrdU and rabbit-anti-FOX3) were diluted in PBS supplemented with 3 % donkey serum and 0.1 % Triton X-100. Incubation was performed overnight at 4 °C. After several rinses in PBS, the sections were incubated with secondary antibodies (anti-rat Alexa Fluor 488, anti-mouse Cy3 and anti-rabbit Alexa Fluor 647)

diluted in PBS supplemented with 3 % donkey serum and 0.1 % Triton X-100 at room temperature for 4 h. They were then washed in PBS, after which 4′,6-diamidino-2-phenylindole (DAPI) staining was performed for 10 min using DAPI diluted 1:2000 in PBS. After a final wash with PBS, the sections were mounted on glass slides and coverslipped with Aqua-Poly/Mount (Polysciences Europe GmbH). Every sixth section (240 µm apart) was counted in the complete ventral dorsal extent of the dentate gyrus, at 40x magnification using a Zeiss Apotome microscope. Results were multiplied by 6 in order to obtain the total number of positive cells within the dentate gyrus region of each brain.

Standard fluorescence immunohistochemistry

For all other fluorescence immunohistochemistry, sections were first incubated for 60 min at room temperature in 0.1 M PBS containing 10 % normal donkey serum (NDS; Sigma-Aldrich) and 0.2 % Triton X-100. The blocking solution was replaced with fresh solution containing 3 % NDS, 0.2 % Triton X-100 and primary antibodies. Following incubation for 36 h at 4 °C the sections were washed with PBS and incubated for 4 h at room temperature in blocking solution containing the appropriate DyLight secondary antibodies (1:500; Dianova). After washing with PBS, the sections were mounted onto slides and coverslipped with 2.5 % PVA-DABCO.

Whole slide imaging

A one-in-three series of coronal cryosections were acquired using a wide-field microscope specifically equipped for fast and automated image acquisition (Zeiss AxioObserver with AxioCam MRm and ZEN blue 2012 software). Preview images of every slide were acquired in phase-contrast using a 2.5x objective. Individual sections were marked, the tile-region adjusted and the sections imaged using a 10x objective. Subsequently, image brightness and contrast were adjusted for display.

Analyses of LPA_1-GFP^+ phenotypes

Images were captured with a laser scanning microscope (Zeiss LSM 780) using a 20x objective (Plan-APOChromat NA 0,8) and 10x objective (Plan-APOChromat NA 0,45 for Figure 2B) using the sequential scanning mode and checking each fluorophore for bleach-through to neighboring channels. Linear unmixing was performed using Zeiss software (ZEN black 2012), using tissue sections of Nestin-Cyan nuclear and LPA_1-GFP mice to generate the emission spectra of the single fluorophores.

Maximum intensity projections were also performed using the ZEN black software. Images were processed with ImageJ (Version 1.47) and Photoshop CS5, and, if necessary, only general brightness/contrast enhancements of the entire image were applied with no further manipulations. Some image sizes were adapted using bicubic interpolation to fit into the figures and in order to adjust the panels to the requested format.

For quantification of LPA_1-GFP co-localization with other makers, 800 GFP^+ cells over 4 animals for each antibody combination were imaged and phenotyped.

Fluorescence activated cell sorting and *in vitro* cell culture

Nestin-GFP or LPA_1-GFP mice (8 weeks old; 8 per experiment) were killed, their brains immediately removed, and the dentate gyrus microdissected (Hagihara et al., 2009). The tissue was enzymatically digested using a Neural Tissue Dissociation Kit (Miltenyi) according to the manufacturer's instructions. Following a final wash in Hank's balanced salt solution (HBSS) (PAA; GE Healthcare) the pellet was resuspended in 1 ml of HBSS and filtered through a 40 µm cell sieve (Falcon; BD Biosciences). Cells were stained with a prominin-1 specific antibody (1:200, 13A4-phycoerythrin (PE); eBioscience) and/or EGF-647 (1:100, Molecular Probes) for 30 min at 4 °C. Prior to adding the prominin-1-PE or EGF-647, a small proportion of the cells were removed and stained with an isotype control (rat IgG1-PE; eBioscience) as a control for non-specific staining. The cells

were finally washed in 10 ml HBSS before being resuspended in 1 ml of HBSS. They were then analyzed using a FACS Aria III cell sorter (BD Biosciences). Dead cells were excluded by staining with propidium iodide (1 μg/ml). The WT live fraction consisted of all cells collected from a wild-type animal following exclusion of the dead cells using the dye propidium iodide. Sorted populations of cells were collected directly into neurosphere growth medium and each population was plated into 48 wells of a 96-well plate as described elsewhere (Walker and Kempermann, 2014). Approximately 16 h after sorting the cells were counted in at least 6 wells, and the average cell number per well was determined.

FACS analysis of DG niche composition

To determine the cellular composition of the dentate gyrus, cells were isolated from LPA_1-GFP mice as described above. Using flow cytometry we analyzed the percentage of cells that were neurons ($NeuN^+$), astrocytes ($GFAP^+$), microglia ($CD11b^+$), neuroblasts ($PSA\text{-}NCAM^+$) and precursor cells ($LPA_1\text{-}GFP^+$). For the intracellular markers (NeuN and GFAP) the cells were first fixed with 0.4 % PFA for 15 mins at room temperature. Following a wash with PBS, the cells were resuspended in PBS containing 1 % BSA and 0.1 % saponin and the primary antibody (NeuN 1:100 or GFAP 1:500) added and incubated for 30 mins at 4 °C. Following another PBS wash the cells were resuspended in buffer containing secondary antibody (1:500; anti-mouse Cy5 or anti-rabbit Alexa Flour647) for 20 mins at 4 °C in the dark. The cells were then washed with PBS and resuspended in 500 μl PBS and filtered through a 40 μm sieve before being analysed using a AriaIII flow cytometer (BD Biosciences). For the surface antibodies the cells were stained in PBS containing (1:200; CD11b-PE or PSA-NCAM-PE) for 30 mins at 4 °C in the dark, washed with PBS, resuspended in PBS and filtered through a 40 μm sieve. The appropriate secondary only or isotype controls were used to set the background gates for analysis.

LPA and cytokine neurosphere cultures

For the *in vitro* neurosphere experiments, primary dentate gyrus cells were isolated as described above and plated at a density of one dentate gyrus per 96 well plate. This is considered to be a clonal density as it gives rise to an average of approximately one neurosphere per well. Immediately prior to plating, the appropriate compounds were added to the cell suspensions: LPA (18:1 1-oleoyl-2-hydroxy-sn-glycero-3-phosphate, 10 μM; Avanti Polar Lipids) the LPA_1 antagonist DGPP (8:0 dioctanoylglycerol pyrophosphate, 50 μM; Avanti Polar Lipids), KCl (15 mM), CXCL1 (3 ng/ml or 30 ng/ml; R & D Systems), CXCL2 (0.1 ng/ml, 1 ng/ml, or 10 ng/ml; R & D Systems) or CCL8 (10 ng/mL or 100 ng/ml; BioLegend). Following 10 days in culture (37 °C / 5% CO_2) neurospheres were counted and their diameter measured using an inverted light microscope fitted with an ocular grarticule.

Neurosphere passaging and differentiation

Primary hippocampal neurospheres were passaged by removing 150 μl of the medium from wells containing single large neurospheres, and treating with 100 μl of 0.05 % trypsin-EDTA (Gibco) for 3 min at room temperature, followed by washing with 100 μl of trypsin inhibitor (0.125 mg/ml trypsin inhibitor plus 0.01 mg/ml DNaseI) in DMEM. The neurospheres were mechanically triturated until dissociated, then replated in 24-well plates in 2 ml of complete medium. Neurospheres were passaged every 10 d by removing the medium containing the neurospheres from the plates and centrifuging at 100 rcf for 7 min. The supernatant was then decanted, and the neurospheres were incubated in 1 ml of 0.05 % trypsin-EDTA for 3 min at room temperature. After the addition of an equal volume of trypsin inhibitor, the neurospheres were centrifuged at 100 rcf for 7 min and the supernatant was removed. Cells were mechanically triturated in 500 μl of complete medium, and trypan blue staining was used to evaluate the number of cells, both viable and the total number, on a hemocytometer. The passaged cells were then replated with complete medium at a density of 1×10^4 cells/cm^2 in tissue culture flasks (Nalge Nunc International) or tissue culture plates (Falcon; BD

Biosciences) as appropriate. For differentiation, neurospheres were plated onto PDL and laminin-coated coverslips in DMEM/F-12 Basal Medium containing mouse NeuroCult NSC Proliferation Supplements without growth factors. The neurospheres were allowed to differentiate for 8 d in humidified 5 % CO_2 until flattened and adherent. The differentiated neurospheres were then fixed with 4 % PFA in 0.1 M PBS at room temperature for 30 min. After washing with PBS, they were stained for either the neuronal markers βIII-tubulin or Map2ab, the astrocytic marker glial fibrillary acidic protein (GFAP), the oligodendrocyte marker O4 or the precursor cell antigen Nestin, with a DAPI counterstain to visualize the nuclei.

Adherent precursor cell line initiation and passaging

The primary cells from each sorted population were plated into one well of a 24-well plate (Falcon; BD Biosciences) that had been coated with PDL (10 mg/ml) and laminin (10 mg/ml) in 2 ml of growth medium. The growth medium consisted of Neurobasal medium (Gibco, Life Technologies), supplemented with 2 % B27 (Invitrogen), 1X GlutaMAX (Life Technologies) and 50 units/ml penicillin/streptomycin (Life Technologies). The following growth factors were also included: 20 ng/ml EGF and 20 ng/ml FGF-2. The growth medium was changed every 2-3 d and the cells were passaged when they reached approximately 80 % confluency.

Immunostaining of neurospheres and adherent cultures

The differentiated neurospheres or adherent cultures were fixed with 4 % PFA (Sigma-Aldrich) in 0.1 M PBS at room temperature for 20 min. After washing with PBS, the cells were incubated in blocking solution (10 % normal donkey serum in 0.1 M PBS containing 0.2 % Triton X-100) for 60 min at room temperature. The cells were then incubated in fresh blocking solution containing mouse monoclonal βIII-tubulin antibody plus rabbit GFAP antibody for 60 min at room temperature. The cells were washed three times with PBS and incubated in fresh blocking solution containing donkey anti-mouse Cy3 antibody (1:1000; Jackson ImmunoResearch), DyLight 488 donkey anti-rabbit antibody (1:1000; Dianova) and DAPI (1:5000; Sigma-Aldrich) for 30 min at room temperature. Following another three PBS washes, the slides were mounted using fluorescence mounting medium (DakoCytomation) before being viewed at 20x magnification on a Zeiss Apotome microscope.

Next generation sequencing

Three populations of primary DG cells; "proliferative precursor cells" (LPA_1-$GFP^+EGFR^+Prominin1^+$), "non-proliferative precursor cells" (LPA_1-GFP^+EGFR^+prominin-1^-, LPA_1-GFP^+EGF^-prominin-1^+ and LPA_1-GFP^+EGFR^-prominin-1^-) and "niche cells" (LPA_1-GFP^-) were isolated by FACS and pools of approximately 1000 cells were used for RNA extraction using the RNeasy micro kit (Qiagen). After elution in 10 µl of RNase free water, 5 µl was used for cDNA synthesis using SmartScribe reverse transcriptase (Clontec), a universally tailed poly-dT primer and a template switching oligonucleotide. This was followed by 12 cycles of amplification of the purified cDNA with the Advantage 2 DNA Polymerase. After ultrasonic shearing of the amplified cDNA (Covaris S2) samples were subjected to standard Illumina fragment library preparation using the NEBnext chemistries (New England Biolabs). The libraries were subsequently finalized by a universally primed PCR amplification of 15 cycles. Libraries were purified using XP beads (Beckman Coulter), quantified by qPCR (KAPA Biosysytems) and subjected to Illumina 75 bp single end sequencing on the Illumina HiSeq 2000 platform providing on average 35 Mio reads per sample. Reads were mapped to the latest mouse genome build (mm10) using the STAR algorithm (Dobin et al., 2013). A novel algorithm, FPKEM (https://pypi.python.org/pypi/fpkem), was used to obtain counts of fragments per kilobase of expressed exonic sequence per million reads. Raw fpkem data were shifted by the addition of a constant (= 1) and then log_2-transformed.

Transcriptome analysis

All analyses were performed in R (http://www.R-project.org/). An ANOVA filter (Benjamini-

Hochberg adjusted $p < 0.05$) was used to select transcripts that were significantly different between the populations. Stem and precursor cell-specific transcripts were then defined by a 4-fold ($\log_2$ difference of 2) increase in expression between the groups; i.e. either higher in stem cells vs. niche cells and higher in progenitor cells vs. niche cells (precursor cell-specific) or higher in stem cells vs. niche cells and higher in stem cells vs. progenitor cells (stem cell-specific). Gene Ontology enrichment (Ashburner et al., 2000) was carried out using the topGO package (Alexa & Rahnenfuhrer, 2010) and visualized with the help of REViGO (http://revigo.irb.hr/; (Supek et al., 2011)). REViGO was carried out with a sematic similarity threshold of 0.7 using the method of Lin (1998). KEGG enrichment (Kanehisa and Goto, 2000) was done with the clusterProfiler package (Yu et al., 2012). The STRING network graph was exported from the STRING web interface (http://string-db.org/) and visualized using Cytoscape (http://www.cytoscape.org/).

Principal component analysis was performed using the package *prcomp*. Figure 5A was reconstructed using data and code from a published single cell sequencing study (Shin et al., 2015). Briefly, data for all genes in individual cells were subjected to principal component decomposition and PC1 and PC2 were plotted. Five cell subtypes (S1–S5) were identified by clustering and colored differently on the plot (see original paper and accompanying Supplemental Data for details; Shin *et al.*, 2015). To compare our data with that study, we first retrieved expression data from the Shin *et al.* dataset which matched our lists of genes enriched in the proliferative and non-proliferative $LPAR^+$ populations (Table S1; matched by gene symbol, as different IDs were used in the two studies). A principal component analysis was then performed using each of these two new data subsets and an eigengene was calculated from the first principal component with the sign adjusted to positively correlate with the mean gene expression for each cell and scaled so that the minimum value was equal to 0. This eigengene was plotted as a bar graph in which data were pooled for all the cells in each of the defined subtypes (S1–S5), and the expression level of the eigengene (red high; yellow low) was used to color the PCA plot from figure 5A to show how gene expression in the two $LPAR^+$ cell types corresponded to the scheme of cell subtypes described in the Shin *et al.* study.

LPA signaling, protein preparation and western blot analysis

Adherent precursor cultures (passage 5) derived from the LPA_1-GFP^+ population were grown to approximately 80 % confluency in 6 well plates then transferred to mitogen-free medium for 24 h. LPA (25 μM) was added, and the cells were incubated for 2, 5, 10, 30 or 60 min at 37 °C. For the ex vivo experiments primary dentate gyrus cells were isolated and treated with either PBS or LPA (25 μM) for 10 mins. Following the appropriate LPA stimulation, cells were washed once in ice cold PBS and lyzed immediately on ice in 150 μl lysis buffer (10 mM Tris, 150 ml NaCl, 5 mM EDTA, 1 % NP40, 0.1 % SDS, 1 × complete protease inhibitors (Roche), 1 % phosphatase inhibitor cocktail 3 (Sigma) pH 7.5 for 20 min and clarified by centrifugation at 16,000 x g for 10 min at 4 °C. Lysates were separated on 4-12 % NuPage gels and transferred to polyvinylidene fluoride membranes. The following antibodies were used rabbit anti-AKT (1:2000; Cell Signaling), rabbit anti-phospho AKT-S473 (1:2000; Cell Signaling) or mouse anti-phospho Erk1/2 (1:2000; Cell Signaling). Immunoreactive bands were detected using either donkey anti-rabbit HRP or goat anti-mouse (1:50000; Jackson ImmunoResearch Laboratories) secondary antibodies and the SuperSignal West Dura Chemiluminescent Substrate (Thermo Scientific) followed by exposure to Hyperfilm (GE Healthcare).

Data analysis

Data analysis (with the exception of the next generation sequencing analysis) was performed using Prism software (Version 4.0c, GraphPad Software, Inc). Results were expressed as mean ± standard error of the mean (SEM). Statistical significance was determined using one-way ANOVA with a Tukey's *post hoc* test or student's t-tests as appropriate. The level of conventional statistical significance was set at $p < 0.05$.

Supplemental References

Alexa, A. and Rahnenfuhrer, R. (2010). topGO: topGO: Enrichment analysis for Gene Ontology. R package version 2.16.0.

Ashburner, M., Ball, C.A., Blake, J.A., Botstein, D., Butler, H., Cherry, J.M., Davis, A.P., Dolinski, K., Dwight, S.S., Eppig, J.T.*, et al.* (2000). Gene ontology: tool for the unification of biology. The Gene Ontology Consortium. Nat Genet *25*, 25-29.

Dobin, A., Davis, C.A., Schlesinger, F., Drenkow, J., Zaleski, C., Jha, S., Batut, P., Chaisson, M., and Gingeras, T.R. (2013). STAR: ultrafast universal RNA-seq aligner. Bioinformatics *29*, 15-21.

Encinas, J.M., and Enikolopov, G. (2008). Identifying and quantitating neural stem and progenitor cells in the adult brain. Methods Cell Biol *85*, 243-272.

Gong, S., Zheng, C., Doughty, M.L., Losos, K., Didkovsky, N., Schambra, U.B., Nowak, N.J., Joyner, A., Leblanc, G., Hatten, M.E.*, et al.* (2003). A gene expression atlas of the central nervous system based on bacterial artificial chromosomes. Nature *425*, 917-925.

Hagihara, H., Toyama, K., Yamasaki, N., and Miyakawa, T. (2009). Dissection of hippocampal dentate gyrus from adult mouse. J Vis Exp.

Kanehisa, M., and Goto, S. (2000). KEGG: kyoto encyclopedia of genes and genomes. Nucleic Acids Res *28*, 27-30.

Shin, J., Berg, D.A., Zhu, Y., Shin, J.Y., Song, J., Bonaguidi, M.A., Enikolopov, G., Nauen, D.W., Christian, K.M., Ming, G.L.*, et al.* (2015). Single-Cell RNA-Seq with Waterfall Reveals Molecular Cascades underlying Adult Neurogenesis. Cell Stem Cell *17*, 360-372.

Supek, F., Bosnjak, M., Skunca, N., and Smuc, T. (2011). REVIGO summarizes and visualizes long lists of gene ontology terms. PLoS One *6*, e21800.

Walker, T.L., and Kempermann, G. (2014). One mouse, two cultures: isolation and culture of adult neural stem cells from the two neurogenic zones of individual mice. J Vis Exp.

Yamaguchi, M., Saito, H., Suzuki, M., and Mori, K. (2000). Visualization of neurogenesis in the central nervous system using nestin promoter-GFP transgenic mice. Neuroreport *11*, 1991-1996.

Yu, G., Wang, L.G., Han, Y., and He, Q.Y. (2012). clusterProfiler: an R package for comparing biological themes among gene clusters. OMICS *16*, 284-287.

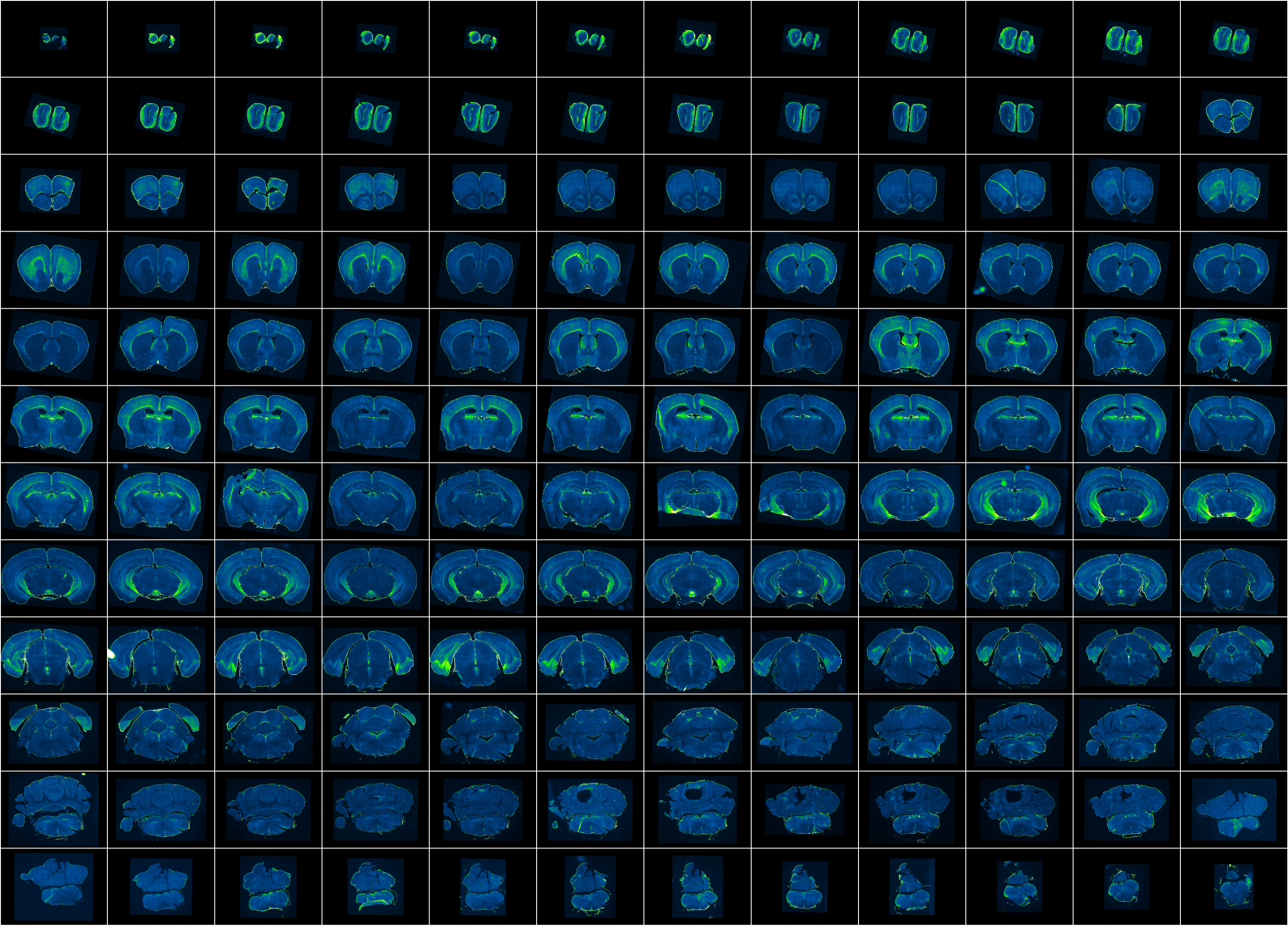

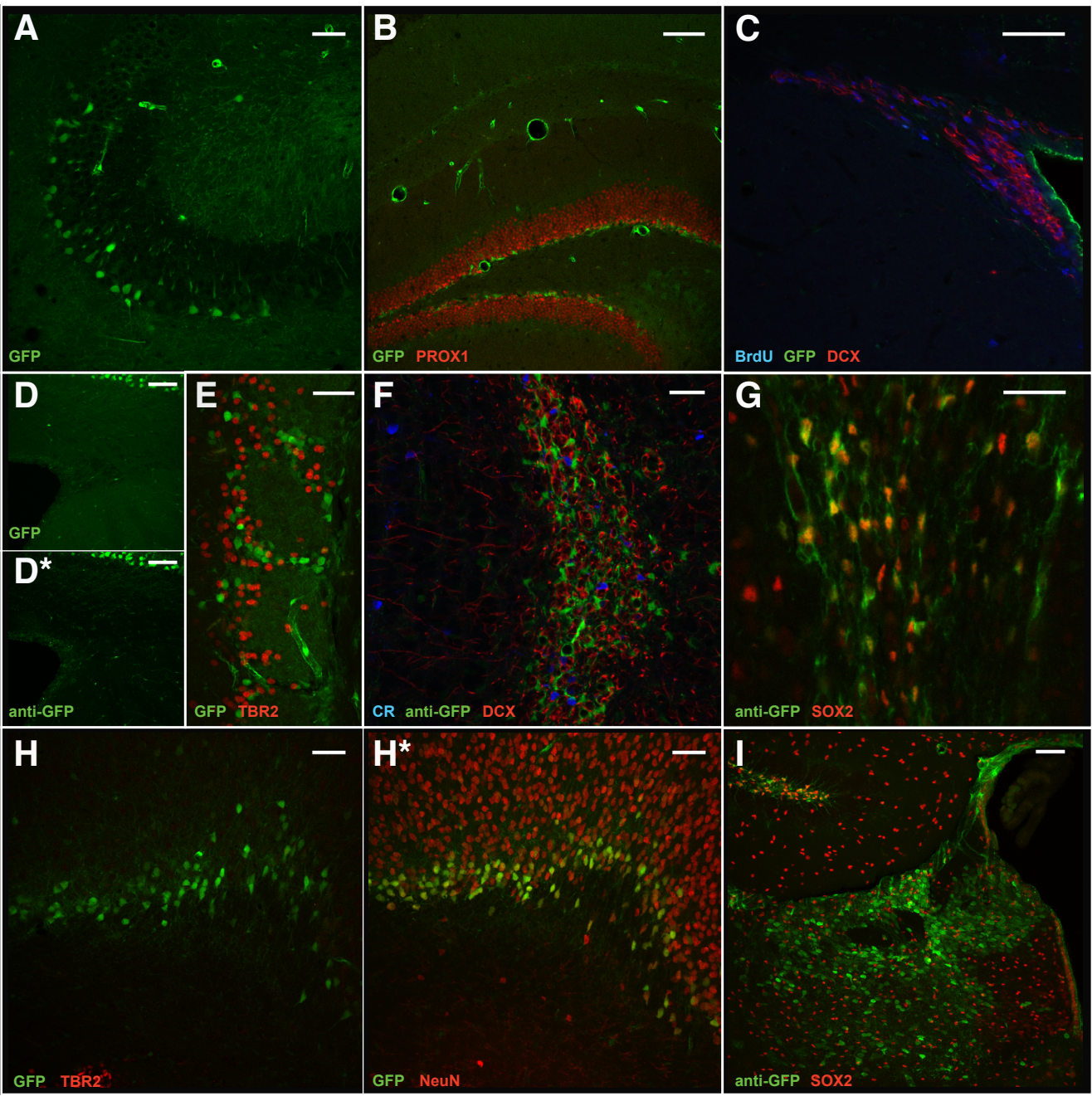
A
GFP
B
GFP PROX1
C
BrdU GFP DCX
D
GFP
D*
anti-GFP
E
GFP TBR2
F
CR anti-GFP DCX
G
anti-GFP SOX2
H
GFP TBR2
H*
GFP NeuN
I
anti-GFP SOX2

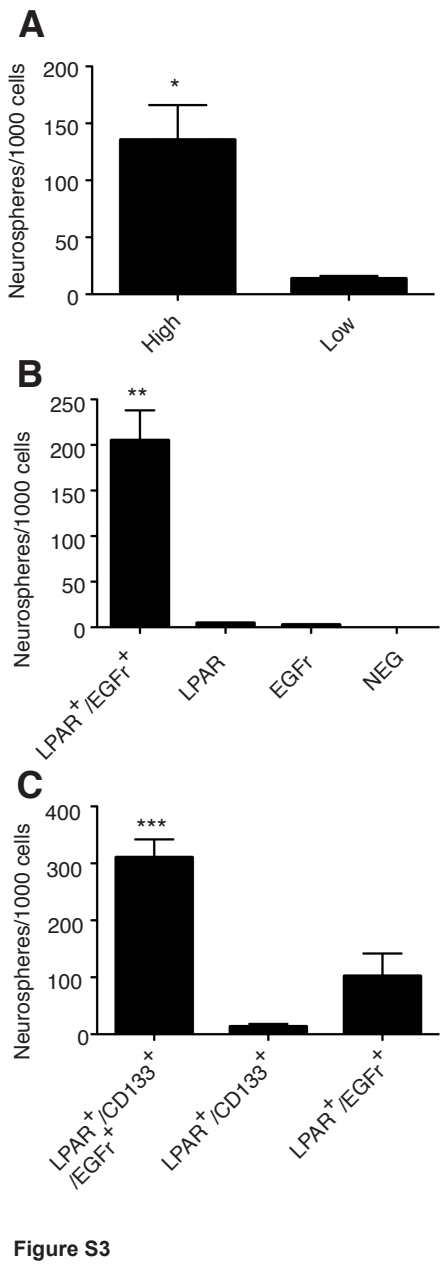
A
Neurospheres/1000 cells
200
150
100
50
0
*
High
Low
B
Neurospheres/1000 cells
250
200
150
100
50
0
**
LPAR+/EGFr+
LPAR
EGFr
NEG
C
Neurospheres/1000 cells
400
300
200
100
0
***
LPAR+/CD133+/EGFr+
LPAR+/CD133+
LPAR+/EGFr+

Figure S3

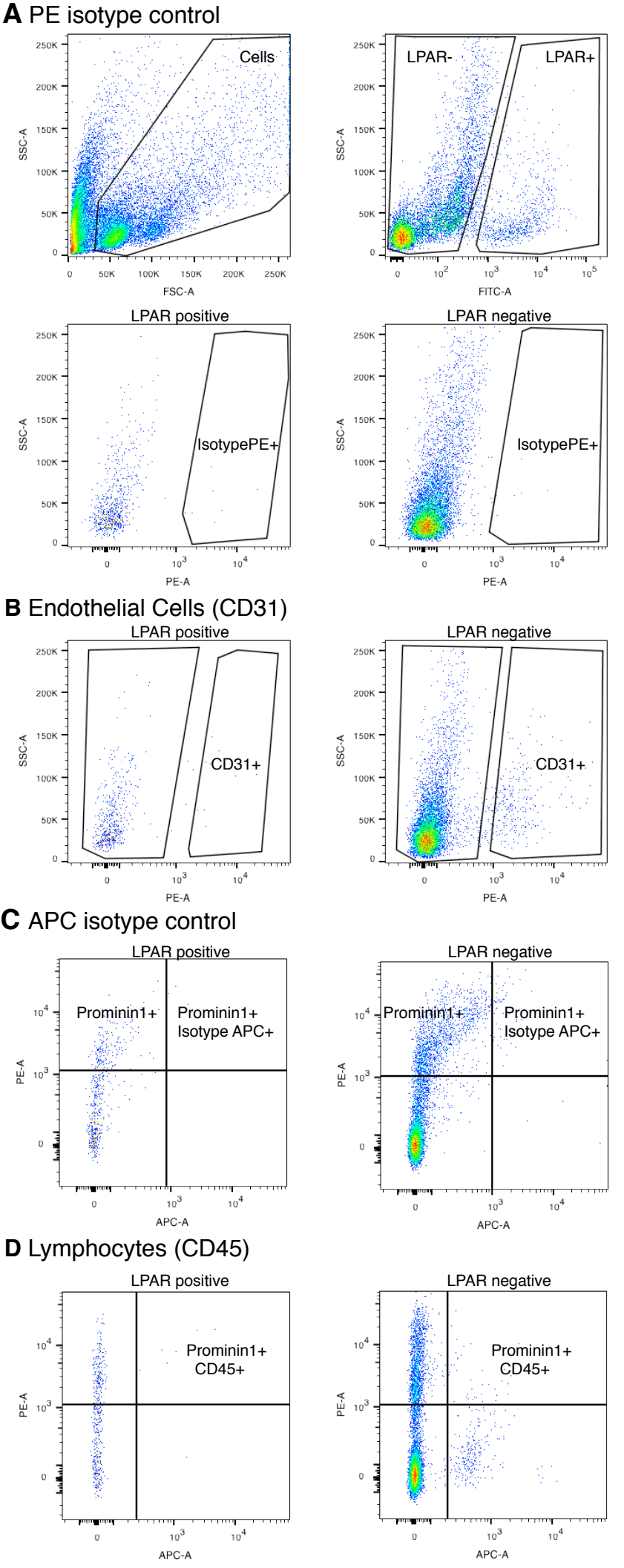
A PE isotype control
Cells
SSC-A
FSC-A
LPAR-
LPAR+
FITC-A
LPAR positive
IsotypePE+
PE-A
LPAR negative
IsotypePE+
PE-A
B Endothelial Cells (CD31)
LPAR positive
CD31+
PE-A
LPAR negative
CD31+
PE-A
C APC isotype control
LPAR positive
Prominin1+
Prominin1+
Isotype APC+
PE-A
APC-A
LPAR negative
Prominin1+
Prominin1+
Isotype APC+
PE-A
APC-A
D Lymphocytes (CD45)
LPAR positive
Prominin1+
CD45+
PE-A
APC-A
LPAR negative
Prominin1+
CD45+
PE-A
APC-A

Figure S4

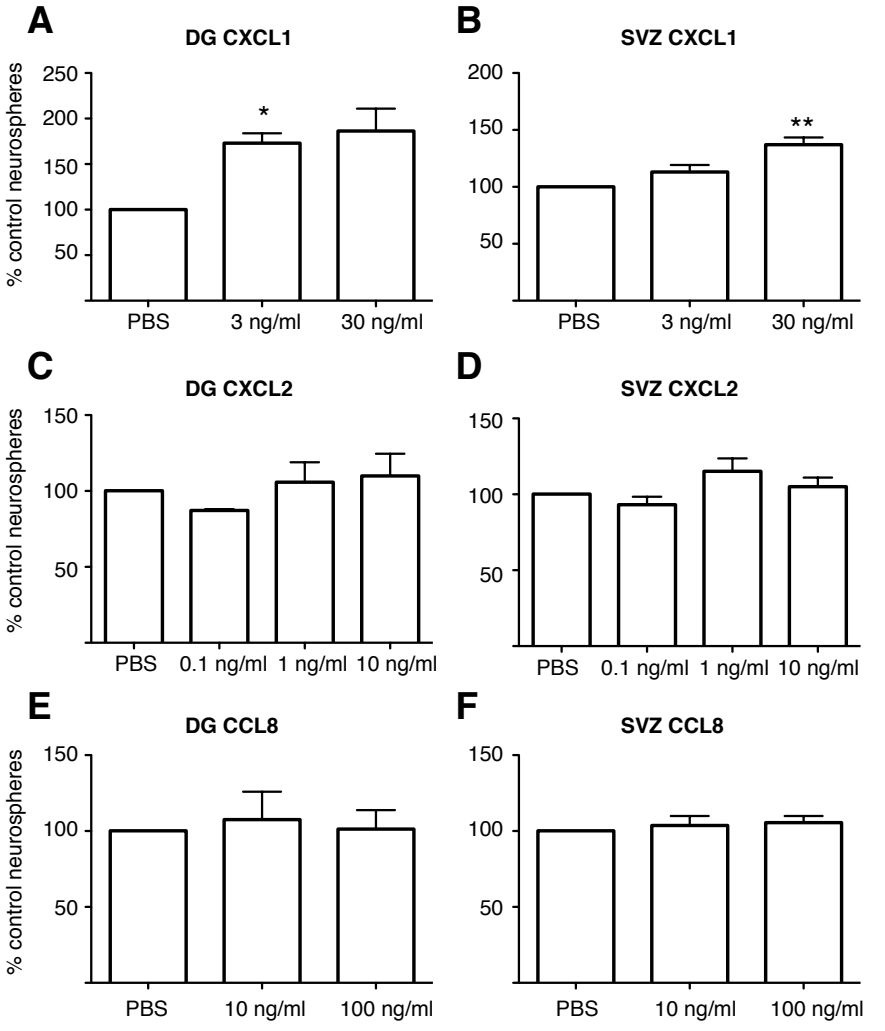
A
DG CXCL1
% control neurospheres
250
200
150
100
50
*
PBS
3 ng/ml
30 ng/ml
B
SVZ CXCL1
200
150
100
50
**
PBS
3 ng/ml
30 ng/ml
C
DG CXCL2
% control neurospheres
150
100
50
PBS
0.1 ng/ml
1 ng/ml
10 ng/ml
D
SVZ CXCL2
150
100
50
PBS
0.1 ng/ml
1 ng/ml
10 ng/ml
E
DG CCL8
% control neurospheres
150
100
50
PBS
10 ng/ml
100 ng/ml
F
SVZ CCL8
150
100
50
PBS
10 ng/ml
100 ng/ml

Figure S5

Supplemental Table 3.
Gene Ontology enrichment for precursor cells.

GO.ID	Term	Annotated	Significant	Expected	Fisher	adjP
GO:0007067	mitosis	171	32	4.74	2.80×10^{-18}	3.90×10^{-15}
GO:0051301	cell division	311	42	8.63	3.00×10^{-18}	3.90×10^{-15}
GO:0000280	nuclear division	227	36	6.3	5.10×10^{-18}	3.90×10^{-15}
GO:0048285	organelle fission	241	37	6.69	5.10×10^{-18}	3.90×10^{-15}
GO:0007049	cell cycle	582	57	16.15	6.00×10^{-18}	3.90×10^{-15}
GO:0022402	cell cycle process	426	46	11.82	4.50×10^{-16}	2.40×10^{-13}
GO:0006259	DNA metabolic process	359	41	9.96	3.40×10^{-15}	1.50×10^{-12}
GO:0000278	mitotic cell cycle	298	35	8.27	2.00×10^{-13}	8.10×10^{-11}
GO:0007059	chromosome segregation	84	19	2.33	8.10×10^{-13}	2.90×10^{-10}
GO:0000819	sister chromatid segregation	37	12	1.03	1.50×10^{-10}	5.00×10^{-8}
GO:1902589	single-organism organelle organization	777	53	21.56	2.80×10^{-10}	8.20×10^{-8}
GO:0000070	mitotic sister chromatid segregation	32	11	0.89	4.50×10^{-10}	1.20×10^{-7}
GO:0090304	nucleic acid metabolic process	1737	87	48.19	1.40×10^{-9}	3.60×10^{-7}
GO:0000226	microtubule cytoskeleton organization	159	21	4.41	2.20×10^{-9}	5.10×10^{-7}
GO:0007017	microtubule-based process	233	25	6.46	5.00×10^{-9}	1.10×10^{-6}
GO:0006260	DNA replication	100	16	2.77	1.20×10^{-8}	2.40×10^{-6}
GO:0006996	organelle organization	1167	64	32.38	2.10×10^{-8}	3.90×10^{-6}
GO:0007051	spindle organization	35	10	0.97	2.20×10^{-8}	3.90×10^{-6}
GO:0006807	nitrogen compound metabolic process	2423	105	67.23	4.20×10^{-8}	7.00×10^{-6}
GO:0006974	cellular response to DNA damage stimulus	265	25	7.35	6.80×10^{-8}	1.10×10^{-5}
GO:0006725	cellular aromatic compound metabolic process	2231	98	61.9	9.30×10^{-8}	1.40×10^{-5}
GO:1901360	organic cyclic compound metabolic process	2299	100	63.79	1.00×10^{-7}	1.50×10^{-5}
GO:0006281	DNA repair	164	19	4.55	1.20×10^{-7}	1.60×10^{-5}
GO:0051276	chromosome organization	353	29	9.79	1.20×10^{-7}	1.60×10^{-5}
GO:0034641	cellular nitrogen compound metabolic process	2300	99	63.82	2.20×10^{-7}	2.80×10^{-5}
GO:0006139	nucleobase-containing compound metabolic process	2181	95	60.51	2.70×10^{-7}	3.40×10^{-5}
GO:0046483	heterocycle metabolic process	2226	96	61.76	3.70×10^{-7}	4.40×10^{-5}
GO:0051726	regulation of cell cycle	293	25	8.13	4.70×10^{-7}	5.50×10^{-5}
GO:0034502	protein localization to chromosome	13	6	0.36	6.20×10^{-7}	6.90×10^{-5}
GO:0010564	regulation of cell cycle process	170	18	4.72	9.70×10^{-7}	1.00×10^{-4}
GO:0007088	regulation of mitosis	42	9	1.17	1.70×10^{-6}	0.00017
GO:0071103	DNA conformation change	81	12	2.25	2.00×10^{-6}	2.00×10^{-4}
GO:0033554	cellular response to stress	519	33	14.4	5.40×10^{-6}	0.00053
GO:0006261	DNA-dependent DNA replication	37	8	1.03	6.00×10^{-6}	0.00056
GO:0030261	chromosome condensation	11	5	0.31	6.30×10^{-6}	0.00058
GO:0043170	macromolecule metabolic process	3038	116	84.29	6.90×10^{-6}	0.00061
GO:0006323	DNA packaging	64	10	1.78	9.00×10^{-6}	0.00078
GO:0051783	regulation of nuclear division	52	9	1.44	1.10×10^{-5}	9.00×10^{-4}
GO:0071840	cellular component organization or biogenesis	1968	83	54.6	1.10×10^{-5}	9.00×10^{-4}
GO:0044260	cellular macromolecule metabolic process	2729	106	75.72	1.30×10^{-5}	0.001
GO:0016043	cellular component organization	1917	81	53.19	1.40×10^{-5}	0.0011
GO:0007346	regulation of mitotic cell cycle	131	14	3.63	1.50×10^{-5}	0.0011
GO:0044770	cell cycle phase transition	131	14	3.63	1.50×10^{-5}	0.0011
GO:0006302	double-strand break repair	55	9	1.53	1.70×10^{-5}	0.0013
GO:0000075	cell cycle checkpoint	71	10	1.97	2.30×10^{-5}	0.0017
GO:0050000	chromosome localization	15	5	0.42	3.80×10^{-5}	0.0026
GO:0051303	establishment of chromosome localization	15	5	0.42	3.80×10^{-5}	0.0026
GO:0044772	mitotic cell cycle phase transition	129	13	3.58	5.50×10^{-5}	0.0037
GO:0071704	organic substance metabolic process	3827	134	106.18	8.00×10^{-5}	0.0052
GO:0000910	cytokinesis	52	8	1.44	8.10×10^{-5}	0.0052
GO:0044238	primary metabolic process	3693	130	102.47	9.60×10^{-5}	0.006
GO:0051302	regulation of cell division	84	10	2.33	0.0001	0.0062
GO:0090068	positive regulation of cell cycle process	69	9	1.91	0.00011	0.0067
GO:0044237	cellular metabolic process	3671	129	101.85	0.00012	0.0071

GO:0007052	mitotic spindle organization	20	5	0.55	0.00017	0.01
GO:0006310	DNA recombination	74	9	2.05	0.00019	0.011
GO:0007093	mitotic cell cycle checkpoint	45	7	1.25	0.00021	0.012
GO:0009262	deoxyribonucleotide metabolic process	12	4	0.33	0.00024	0.013
GO:0051310	metaphase plate congression	12	4	0.33	0.00024	0.013
GO:0007091	metaphase/anaphase transition of mitotic cell cycle	22	5	0.61	0.00028	0.015
GO:0044784	metaphase/anaphase transition of cell cycle	22	5	0.61	0.00028	0.015
GO:0051297	centrosome organization	34	6	0.94	0.0003	0.016
GO:0007010	cytoskeleton organization	404	24	11.21	0.00033	0.017
GO:0071824	protein-DNA complex subunit organization	65	8	1.8	0.0004	0.02
GO:0032886	regulation of microtubule-based process	66	8	1.83	0.00044	0.022
GO:0031023	microtubule organizing center organization	37	6	1.03	0.00048	0.023
GO:0008152	metabolic process	4173	140	115.78	0.00048	0.023
GO:0065004	protein-DNA complex assembly	52	7	1.44	0.00053	0.025
GO:0051983	regulation of chromosome segregation	15	4	0.42	0.00062	0.029
GO:0007126	meiotic nuclear division	72	8	2	0.0008	0.037
GO:0051225	spindle assembly	16	4	0.44	0.00081	0.037
GO:1901988	negative regulation of cell cycle phase transition	56	7	1.55	0.00084	0.037
GO:1901991	negative regulation of mitotic cell cycle phase transition	56	7	1.55	0.00084	0.037
GO:0051321	meiotic cell cycle	74	8	2.05	0.00096	0.042
GO:0070507	regulation of microtubule cytoskeleton organization	58	7	1.61	0.00104	0.045

Supplemental Table 4.
Gene Ontology enrichment for proliferative cells.

GO.ID	Term	Annotated	Significant	Expected	Fisher	adjP
GO:0002376	immune system process	686	39	10.26	5.10×10^{-14}	1.60×10^{-10}
GO:0006950	response to stress	1037	47	15.51	2.60×10^{-13}	4.10×10^{-10}
GO:0006955	immune response	343	26	5.13	3.70×10^{-12}	4.00×10^{-9}
GO:0006952	defense response	360	26	5.39	1.10×10^{-11}	9.00×10^{-9}
GO:0009607	response to biotic stimulus	222	20	3.32	7.30×10^{-11}	4.10×10^{-8}
GO:0009611	response to wounding	303	23	4.53	7.70×10^{-11}	4.10×10^{-8}
GO:0043207	response to external biotic stimulus	209	19	3.13	2.00×10^{-10}	7.90×10^{-8}
GO:0051707	response to other organism	209	19	3.13	2.00×10^{-10}	7.90×10^{-8}
GO:0050896	response to stimulus	2592	72	38.78	2.20×10^{-10}	8.00×10^{-8}
GO:0001562	response to protozoan	16	7	0.24	1.40×10^{-9}	4.60×10^{-7}
GO:0006954	inflammatory response	186	17	2.78	1.80×10^{-9}	5.30×10^{-7}
GO:0098542	defense response to other organism	109	13	1.63	6.70×10^{-9}	1.80×10^{-6}
GO:0051716	cellular response to stimulus	2086	60	31.21	1.00×10^{-8}	2.50×10^{-6}
GO:0009605	response to external stimulus	563	27	8.42	3.90×10^{-8}	9.10×10^{-6}
GO:0042832	defense response to protozoan	15	6	0.22	4.40×10^{-8}	9.50×10^{-6}
GO:0002682	regulation of immune system process	356	20	5.33	2.50×10^{-7}	5.10×10^{-5}
GO:0048584	positive regulation of response to stimulus	553	25	8.27	4.30×10^{-7}	8.20×10^{-5}
GO:0002684	positive regulation of immune system process	211	15	3.16	4.90×10^{-7}	8.80×10^{-5}
GO:0051704	multi-organism process	534	24	7.99	8.60×10^{-7}	0.00015
GO:0070887	cellular response to chemical stimulus	638	26	9.54	1.80×10^{-6}	0.00028
GO:0034097	response to cytokine	175	13	2.62	1.80×10^{-6}	0.00028
GO:0045087	innate immune response	151	12	2.26	2.30×10^{-6}	0.00034
GO:0009617	response to bacterium	133	11	1.99	4.30×10^{-6}	6.00×10^{-4}
GO:0060341	regulation of cellular localization	359	18	5.37	5.50×10^{-6}	0.00074
GO:0007165	signal transduction	1676	46	25.07	7.40×10^{-6}	0.00093
GO:0071345	cellular response to cytokine stimulus	141	11	2.11	7.50×10^{-6}	0.00093
GO:0044763	single-organism cellular process	4283	87	64.07	8.50×10^{-6}	0.001
GO:0008283	cell proliferation	613	24	9.17	9.70×10^{-6}	0.0011
GO:0010033	response to organic substance	701	26	10.49	1.00×10^{-5}	0.0011
GO:0042221	response to chemical	983	32	14.71	1.20×10^{-5}	0.0013
GO:0048518	positive regulation of biological process	1617	44	24.19	1.70×10^{-5}	0.0017
GO:0023056	positive regulation of signaling	433	19	6.48	2.00×10^{-5}	0.002
GO:0023052	signaling	1851	48	27.69	2.10×10^{-5}	0.002
GO:0044700	single organism signaling	1851	48	27.69	2.10×10^{-5}	0.002
GO:0010647	positive regulation of cell communication	436	19	6.52	2.20×10^{-5}	0.002
GO:0006913	nucleocytoplasmic transport	158	11	2.36	2.20×10^{-5}	0.002
GO:0051169	nuclear transport	159	11	2.38	2.40×10^{-5}	0.002
GO:0006606	protein import into nucleus	106	9	1.59	2.70×10^{-5}	0.0022
GO:0044744	protein targeting to nucleus	106	9	1.59	2.70×10^{-5}	0.0022
GO:1902593	single-organism nuclear import	106	9	1.59	2.70×10^{-5}	0.0022
GO:0032880	regulation of protein localization	226	13	3.38	3.00×10^{-5}	0.0023
GO:0009967	positive regulation of signal transduction	407	18	6.09	3.00×10^{-5}	0.0023
GO:0007154	cell communication	1878	48	28.09	3.10×10^{-5}	0.0023
GO:0051170	nuclear import	108	9	1.62	3.10×10^{-5}	0.0023
GO:0048583	regulation of response to stimulus	1135	34	16.98	3.40×10^{-5}	0.0024
GO:0032386	regulation of intracellular transport	166	11	2.48	3.50×10^{-5}	0.0024
GO:0001816	cytokine production	197	12	2.95	3.50×10^{-5}	0.0024
GO:0048522	positive regulation of cellular process	1448	40	21.66	3.50×10^{-5}	0.0024
GO:0032879	regulation of localization	756	26	11.31	3.80×10^{-5}	0.0025
GO:0042742	defense response to bacterium	43	6	0.64	3.80×10^{-5}	0.0025
GO:0001775	cell activation	303	15	4.53	4.20×10^{-5}	0.0026
GO:0046822	regulation of nucleocytoplasmic transport	87	8	1.3	4.30×10^{-5}	0.0027
GO:1902533	positive regulation of intracellular signal transduction	272	14	4.07	5.00×10^{-5}	0.003
GO:0017038	protein import	116	9	1.74	5.50×10^{-5}	0.0033

GO:0033365	protein localization to organelle	207	12	3.1	5.70×10^{-5}	0.0033
GO:0051223	regulation of protein transport	176	11	2.63	6.00×10^{-5}	0.0033
GO:0008219	cell death	731	25	10.94	6.10×10^{-5}	0.0033
GO:0002221	pattern recognition receptor signaling pathway	29	5	0.43	6.10×10^{-5}	0.0033
GO:0002758	innate immune response-activating signal transduction	29	5	0.43	6.10×10^{-5}	0.0033
GO:0016265	death	732	25	10.95	6.20×10^{-5}	0.0034
GO:0051641	cellular localization	927	29	13.87	7.10×10^{-5}	0.0038
GO:0010562	positive regulation of phosphorus metabolic process	320	15	4.79	7.80×10^{-5}	0.004
GO:0045937	positive regulation of phosphate metabolic process	320	15	4.79	7.80×10^{-5}	0.004
GO:0002218	activation of innate immune response	31	5	0.46	8.60×10^{-5}	0.0043
GO:0050776	regulation of immune response	186	11	2.78	9.90×10^{-5}	0.0048
GO:0042307	positive regulation of protein import into nucleus	32	5	0.48	0.0001	0.0048
GO:0042306	regulation of protein import into nucleus	73	7	1.09	0.0001	0.0048
GO:0051222	positive regulation of protein transport	98	8	1.47	0.0001	0.0048
GO:0070201	regulation of establishment of protein localization	190	11	2.84	0.00012	0.0056
GO:0071310	cellular response to organic substance	498	19	7.45	0.00013	0.006
GO:0034504	protein localization to nucleus	130	9	1.94	0.00013	0.006
GO:0033157	regulation of intracellular protein transport	102	8	1.53	0.00013	0.006
GO:0042127	regulation of cell proliferation	500	19	7.48	0.00014	0.0062
GO:0051050	positive regulation of transport	263	13	3.93	0.00014	0.0062
GO:0006915	apoptotic process	680	23	10.17	0.00015	0.0065
GO:1900180	regulation of protein localization to nucleus	78	7	1.17	0.00015	0.0065
GO:0051649	establishment of localization in cell	778	25	11.64	0.00017	0.007
GO:0090316	positive regulation of intracellular protein transport	56	6	0.84	0.00017	0.0072
GO:0002757	immune response-activating signal transduction	80	7	1.2	0.00018	0.0074
GO:0035556	intracellular signal transduction	882	27	13.19	0.00019	0.0078
GO:0032388	positive regulation of intracellular transport	81	7	1.21	0.0002	0.0078
GO:0012501	programmed cell death	694	23	10.38	0.0002	0.008
GO:0045321	leukocyte activation	275	13	4.11	0.00022	0.0085
GO:0072594	establishment of protein localization to organelle	139	9	2.08	0.00022	0.0085
GO:0050900	leukocyte migration	83	7	1.24	0.00023	0.0086
GO:0044699	single-organism process	4800	90	71.81	0.00024	0.0088
GO:0001817	regulation of cytokine production	172	10	2.57	0.00024	0.0088
GO:0001934	positive regulation of protein phosphorylation	241	12	3.61	0.00024	0.0089
GO:0042981	regulation of apoptotic process	523	19	7.82	0.00025	0.009
GO:0002252	immune effector process	207	11	3.1	0.00025	0.009
GO:0030595	leukocyte chemotaxis	60	6	0.9	0.00026	0.009
GO:0046824	positive regulation of nucleocytoplasmic transport	39	5	0.58	0.00026	0.0092
GO:0042327	positive regulation of phosphorylation	281	13	4.2	0.00027	0.0095
GO:0006796	phosphate-containing compound metabolic process	1366	36	20.43	0.00028	0.0095
GO:0002764	immune response-regulating signaling pathway	86	7	1.29	0.00028	0.0096
GO:0043067	regulation of programmed cell death	530	19	7.93	0.0003	0.01
GO:0042060	wound healing	117	8	1.75	0.00035	0.012
GO:0034613	cellular protein localization	451	17	6.75	0.00036	0.012
GO:0006793	phosphorus metabolic process	1384	36	20.7	0.00036	0.012
GO:0006110	regulation of glycolysis	10	3	0.15	0.00036	0.012
GO:0048247	lymphocyte chemotaxis	10	3	0.15	0.00036	0.012
GO:0002274	myeloid leukocyte activation	64	6	0.96	0.00036	0.012
GO:0070727	cellular macromolecule localization	453	17	6.78	0.00038	0.012
GO:0002253	activation of immune response	91	7	1.36	0.0004	0.012
GO:0034341	response to interferon-gamma	25	4	0.37	0.00047	0.014
GO:0009987	cellular process	5407	97	80.89	0.00048	0.015
GO:0002237	response to molecule of bacterial origin	94	7	1.41	0.00049	0.015
GO:0019221	cytokine-mediated signaling pathway	94	7	1.41	0.00049	0.015
GO:0048009	insulin-like growth factor receptor signaling pathway	11	3	0.16	0.00049	0.015
GO:0051240	positive regulation of multicellular organismal process	225	11	3.37	0.00052	0.015
GO:0010941	regulation of cell death	558	19	8.35	0.00057	0.016
GO:0051049	regulation of transport	561	19	8.39	0.00061	0.017

GO:0045089	positive regulation of innate immune response	47	5	0.7	0.00064	0.018
GO:0009893	positive regulation of metabolic process	899	26	13.45	0.00064	0.018
GO:0055080	cation homeostasis	195	10	2.92	0.00065	0.018
GO:0046885	regulation of hormone biosynthetic process	12	3	0.18	0.00065	0.018
GO:0097529	myeloid leukocyte migration	49	5	0.73	0.00078	0.021
GO:0050778	positive regulation of immune response	132	8	1.97	0.00078	0.021
GO:0002694	regulation of leukocyte activation	165	9	2.47	0.00078	0.021
GO:0032350	regulation of hormone metabolic process	13	3	0.19	0.00084	0.022
GO:0034502	protein localization to chromosome	13	3	0.19	0.00084	0.022
GO:0006886	intracellular protein transport	278	12	4.16	0.00088	0.023
GO:0030335	positive regulation of cell migration	135	8	2.02	0.0009	0.024
GO:0048285	organelle fission	241	11	3.61	0.00092	0.024
GO:0065008	regulation of biological quality	1076	29	16.1	0.00093	0.024
GO:0006809	nitric oxide biosynthetic process	30	4	0.45	0.00097	0.024
GO:0010564	regulation of cell cycle process	170	9	2.54	0.00097	0.024
GO:0031349	positive regulation of defense response	77	6	1.15	0.00098	0.024
GO:0051249	regulation of lymphocyte activation	137	8	2.05	0.00099	0.024
GO:0006605	protein targeting	171	9	2.56	0.00101	0.024
GO:0006935	chemotaxis	171	9	2.56	0.00101	0.024
GO:0007067	mitosis	171	9	2.56	0.00101	0.024
GO:0042330	taxis	171	9	2.56	0.00101	0.024
GO:0050865	regulation of cell activation	171	9	2.56	0.00101	0.024
GO:0050663	cytokine secretion	52	5	0.78	0.00102	0.024
GO:2000147	positive regulation of cell motility	138	8	2.06	0.00104	0.024
GO:0050789	regulation of biological process	3545	70	53.03	0.00105	0.024
GO:0043470	regulation of carbohydrate catabolic process	14	3	0.21	0.00105	0.024
GO:0043471	regulation of cellular carbohydrate catabolic process	14	3	0.21	0.00105	0.024
GO:0050850	positive regulation of calcium-mediated signaling	14	3	0.21	0.00105	0.024
GO:0072676	lymphocyte migration	14	3	0.21	0.00105	0.024
GO:0007166	cell surface receptor signaling pathway	936	26	14	0.00117	0.027
GO:0040017	positive regulation of locomotion	141	8	2.11	0.00119	0.027
GO:0051272	positive regulation of cellular component movement	141	8	2.11	0.00119	0.027
GO:0050730	regulation of peptidyl-tyrosine phosphorylation	80	6	1.2	0.0012	0.027
GO:0031325	positive regulation of cellular metabolic process	837	24	12.52	0.00122	0.027
GO:0008284	positive regulation of cell proliferation	289	12	4.32	0.00123	0.027
GO:0016482	cytoplasmic transport	289	12	4.32	0.00123	0.027
GO:0000070	mitotic sister chromatid segregation	32	4	0.48	0.00124	0.027
GO:0046209	nitric oxide metabolic process	32	4	0.48	0.00124	0.027
GO:0042246	tissue regeneration	15	3	0.22	0.0013	0.028
GO:0045840	positive regulation of mitosis	15	3	0.22	0.0013	0.028
GO:0051247	positive regulation of protein metabolic process	374	14	5.59	0.00132	0.028
GO:0031401	positive regulation of protein modification process	292	12	4.37	0.00135	0.028
GO:0040011	locomotion	508	17	7.6	0.00138	0.029
GO:0032270	positive regulation of cellular protein metabolic process	334	13	5	0.00139	0.029
GO:0051101	regulation of DNA binding	33	4	0.49	0.00139	0.029
GO:0050731	positive regulation of peptidyl-tyrosine phosphorylation	56	5	0.84	0.00143	0.029
GO:0006979	response to oxidative stress	113	7	1.69	0.00146	0.03
GO:0050801	ion homeostasis	218	10	3.26	0.00152	0.031
GO:0051302	regulation of cell division	84	6	1.26	0.00155	0.031
GO:0065007	biological regulation	3723	72	55.7	0.00158	0.031
GO:0042116	macrophage activation	16	3	0.24	0.00159	0.031
GO:0070373	negative regulation of x 10[RK1 and x 10[RK2 cascade	16	3	0.24	0.00159	0.031
GO:0048878	chemical homeostasis	299	12	4.47	0.00165	0.032
GO:0045787	positive regulation of cell cycle	58	5	0.87	0.00167	0.032
GO:1902582	single-organism intracellular transport	428	15	6.4	0.00171	0.033
GO:0071621	granulocyte chemotaxis	35	4	0.52	0.00174	0.033
GO:0008104	protein localization	764	22	11.43	0.0019	0.036
GO:0045860	positive regulation of protein kinase activity	152	8	2.27	0.00193	0.036

GO:0097530	granulocyte migration	36	4	0.54	0.00194	0.036
GO:0018108	peptidyl-tyrosine phosphorylation	119	7	1.78	0.00197	0.037
GO:0000280	nuclear division	227	10	3.4	0.00206	0.038
GO:0046907	intracellular transport	528	17	7.9	0.00208	0.038
GO:0031347	regulation of defense response	154	8	2.3	0.0021	0.038
GO:0070372	regulation of x 10[RK1 and x 10[RK2 cascade	61	5	0.91	0.0021	0.038
GO:0071216	cellular response to biotic stimulus	61	5	0.91	0.0021	0.038
GO:0000819	sister chromatid segregation	37	4	0.55	0.00215	0.039
GO:0023051	regulation of signaling	1029	27	15.39	0.00216	0.039
GO:0018212	peptidyl-tyrosine modification	121	7	1.81	0.00217	0.039
GO:0060326	cell chemotaxis	90	6	1.35	0.00221	0.039
GO:0010646	regulation of cell communication	1031	27	15.42	0.00223	0.039
GO:0045088	regulation of innate immune response	62	5	0.93	0.00226	0.039
GO:0042446	hormone biosynthetic process	18	3	0.27	0.00226	0.039
GO:0046649	lymphocyte activation	230	10	3.44	0.00226	0.039
GO:0051301	cell division	311	12	4.65	0.00229	0.04
GO:0032147	activation of protein kinase activity	91	6	1.36	0.00234	0.04
GO:0051251	positive regulation of lymphocyte activation	91	6	1.36	0.00234	0.04
GO:0045944	positive regulation of transcription from RNA polymerase II promoter	312	12	4.67	0.00235	0.04
GO:0007049	cell cycle	582	18	8.71	0.00239	0.04
GO:2001237	negative regulation of extrinsic apoptotic signaling pathway	39	4	0.58	0.00261	0.044
GO:0044275	cellular carbohydrate catabolic process	19	3	0.28	0.00265	0.044
GO:0045429	positive regulation of nitric oxide biosynthetic process	19	3	0.28	0.00265	0.044
GO:0051785	positive regulation of nuclear division	19	3	0.28	0.00265	0.044
GO:0042110	T cell activation	160	8	2.39	0.00266	0.044
GO:0002685	regulation of leukocyte migration	40	4	0.6	0.00287	0.047
GO:0072507	divalent inorganic cation homeostasis	128	7	1.91	0.00298	0.049
GO:0051098	regulation of binding	96	6	1.44	0.00306	0.05
GO:0032101	regulation of response to external stimulus	201	9	3.01	0.00308	0.05
GO:0033674	positive regulation of kinase activity	164	8	2.45	0.0031	0.05